

Available online at www.sciencedirect.com

SciVerse ScienceDirect

Energy Procedia 37 (2013) 273 – 284

Energy

Procedia

GHGT-11

Managing n-nitrosopiperazine and dinitrosopiperazine

Nathan A. Fine, Mark J. Goldman, Paul T. Nielsen, Gary T. Rochelle*

The University of Texas at Austin, Department of Chemical Engineering, Luminant Carbon Management Program, 200 E Dean Keeton St. Stop C0400, Austin, TX 78712-1589

Abstract

Formation and decomposition of nitroso-piperazine (NNO) compounds were studied under conditions pertinent to amine scrubbing. Nitrogen dioxide (NO_2) has an overall liquid-side mass transfer coefficient of approximately $10^{-6} \text{ mol/Pa}\cdot\text{m}^2\cdot\text{s}$ at 40°C in 8 m PZ. In an amine scrubber designed to remove 90% CO_2 , over 90% of the NO_2 will be absorbed as nitrite (NO_2^-) or n-nitrosopiperazine (MNPZ). The NO_2^- will travel to the absorber where it will react with PZ to form MNPZ and trace amounts of dinitrosopiperazine (DNPZ). NNO formation is first order in NO_2^- , carbamated amine, and hydronium ions. The NNO will thermally decompose in the stripper. Thermal decomposition is first order in NNO and dependent on PZ concentration and loading. NNO formation from the flue gas NO_2 will balance out with NNO thermal decomposition to give steady state NNO concentrations. The NNO steady state concentration is proportional to the inlet NO_2 . It is inversely proportional to the decomposition rate constant and the volume of the stripper sump. An amine scrubber using a flue gas without NO_x removal will have a steady state MNPZ concentration on the order of 1 mM. Reaching the steady state concentration takes on the order of 10 days. DNPZ concentration will be on the order of 10^{-5} mM, which is undetectable using the methods in this work.

© 2013 The Authors. Published by Elsevier Ltd.
Selection and/or peer-review under responsibility of GHGT

Keywords: Nitrosamine, thermal decomposition, carbon capture, amine scrubbing

* Corresponding author. Tel.: +1-512-471-7230; fax: +1-512-471-7060
E-mail address: gtr@che.utexas.edu

1. Introduction

1.1 *N*-Nitrosopiperazine and Dinitrosopiperazine in carbon capture

Piperazine (PZ) and PZ blends are currently being researched as promising solvents due to their higher working capacity, faster absorption kinetics, and greater resistance to thermal degradation. [1] Unfortunately, as a secondary amine, PZ can be nitrosated to form *n*-nitrosopiperazine (MNPZ) and dinitrosopiperazine (DNPZ), two stable and carcinogenic nitrosamines with a TD50 of 8.7 and 3.6 mg/kg body weight/day respectively. [2–6] Recently, the Norwegian Climate and Pollution Agency has directly addressed nitrosamines in amine scrubbing, restricting total nitrosamine and nitramine levels to 0.3 ng/m³ in air and 4 ng/L in water. [7] Since MNPZ and DNPZ are carcinogenic and restricted chemicals, it is necessary to properly characterize and then minimize their concentrations in amine scrubbing before adopting the technology for carbon capture and storage.

1.2 Formation and decomposition of MNPZ

Figure 1 gives a proposed sequence of processes that determine MNPZ accumulation. MNPZ formation can be traced back to the nitrogen dioxide (NO₂) in the flue gas. Flue gas containing NO_x enters a polishing scrubber where some of the NO₂ can be removed via reaction with sulfite. [8] The remaining NO₂ then enters the absorber where a fraction of it can absorb into the PZ solution as nitrite or undergo a 2-phase reaction with PZ to directly form MNPZ. [9–11] The absorbed nitrite will then travel to the stripper where it nitrosates PZ to form MNPZ. PZ nitrosation has previously been observed under acidic conditions or under basic conditions in the presence of formaldehyde. [12–14] Sun et. al have shown that absorbed CO₂ can also theoretically catalyze nitrosamine formation in a PZ solvent. [15] Oxidative degradation products may also act as nitrosating agents for amine scrubbing, [16] but flue gas NO₂ is likely to be a more important precursor to nitrosamine formation in amine scrubbing. Once in the stripper, MNPZ will thermally decompose to not yet identified byproducts. MNPZ formation from flue gas NO₂ and MNPZ thermal decomposition will balance out to eventually give a stable steady-state concentration of MNPZ.

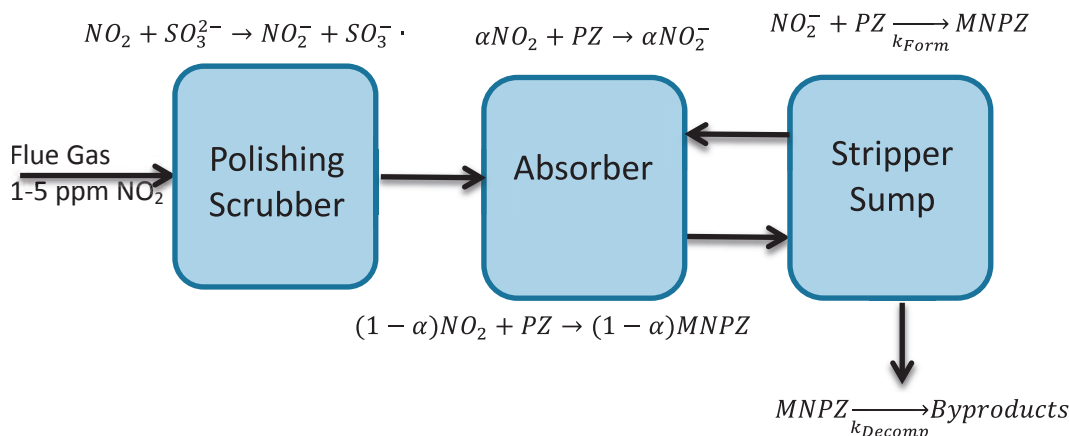


Fig 1: MNPZ formation and decomposition in amine scrubbing

2. NO₂ Absorption

2.1 Experimental Method

Mass transfer of NO₂ into the amine solvent was modelled using the rate based equation for NO₂ flux (Equations 1 & 2).

$$N_{NO_2} = K_g * P_{NO_2} = \frac{\Delta \dot{N}_{O_2}}{A} \quad (1)$$

$$\frac{1}{K_g} = \frac{1}{k_g} + \frac{1}{k'_g} \quad (2)$$

The K_g for NO₂ absorption was measured for 8 m PZ at 0.2–0.4 mol CO₂/mol alkalinity using a wetted wall column and a method previously developed by Dugas. [17] The k'_g was extracted from K_g using correlations for k_g specific to the geometry of the wetted wall column; for every experiment, k'_g was the dominant mass transfer coefficient. Conditions for the inlet gas stream are shown below (Table 1). The outlet gas composition was measured using a hot gas FTIR.

Table 1: Gas Stream Conditions

Condition	Range
Temperature (°C)	20–60
Pressure (psig)	20–40
Flow Rate (SLPM)	2
NO ₂ (ppm)	50–300
CO ₂ (%)	0–4
N ₂ (%)	95–99

2.2 NO₂ Absorption Results

Values for k'_g are plotted as a function of CO₂ loading and temperature in Figure 2. The k'_g has a slight temperature dependence with an activation energy of 13±5 kJ/mol. There is also a small k'_g dependence on loading, but it is much smaller than the loading dependence seen for CO₂ absorption. [17] The fraction of NO₂ absorbed in the absorber is given by Equations 3 and 4 where N_{OG} is the number of overall gas phase transfer units.

$$\frac{N_{O_2 \text{ absorbed}}}{N_{O_2 \text{ Flue}}} = (1 - e^{-N_{OG}}) \quad (3)$$

$$N_{OG} = \frac{K_g * A_{\text{total}}}{G} \quad (4)$$

NO₂ absorption varies from 91% to 99.9% over the entire range of k'_g measured and at a typical A/G of 3.3*10⁶ s·Pa·m²/mol. Thus for a PZ solvent, it is prudent to assume all of the NO₂ will absorb either as MNPZ or as NO₂⁻.

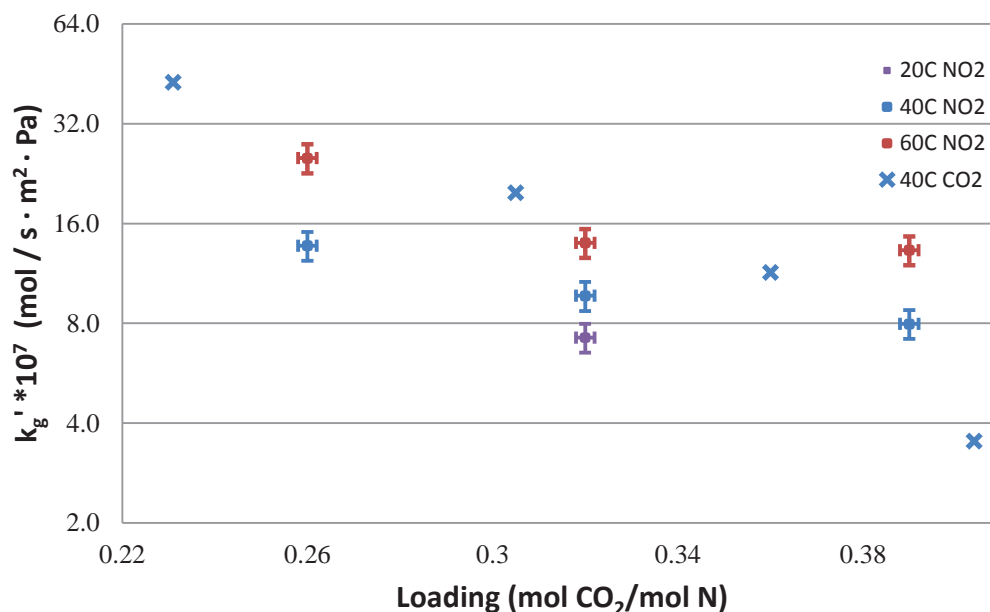


Fig. 2: k'_g of NO₂ in 8 m PZ compared to CO₂ k'_g [17]

3. Formation of MNPZ from NO₂⁻

Previous research suggests that up to half of the NO₂ could directly nitrosate PZ from the gas phase; the balance of the NO₂ will absorb as nitrite. [10] The absorbed nitrite will enter the stripper sump where it will rapidly nitrosate piperazine. PZ nitrosation was measured using Swagelok thermal cylinders heated at 50 to 135 °C. PZ nitrosation was found to be first order in nitrite over a wide range of temperature and PZ concentration. The pseudo-first order rate constant with respect to nitrite was measured at 0.1–8 m PZ, CO₂ loading varying from 0.1–0.4 mol CO₂/mol alkalinity, and 50–135 °C. In a set of experiments, the pH was carefully controlled using a phosphate buffer. Nitrosation was found to be first order in nitrite, carbamated PZ species (PZCOO⁻) as determined by the total CO₂ added, and hydronium ions (H⁺). [18] The experimental kinetics can be explained by a mechanism previously suggested in theoretical research on NDMA formation (Figure 3). [15] The temperature dependence fits an Arrhenius model with an activation energy of 84 kJ/mol and a rate constant of $8.5 \times 10^{-3} \text{ M}^{-2} \text{ s}^{-1}$ at 100 °C (Figure 4). [18] Error in the rate constant can be attributed to CO₂ speciation into bicarbonate (HCO₃⁻) instead of a PZCOO⁻. Nitrite scavenging will not necessarily be a viable strategy to inhibit nitrosamine formation since nitrosation might occur directly in the absorber as well as in the stripper.

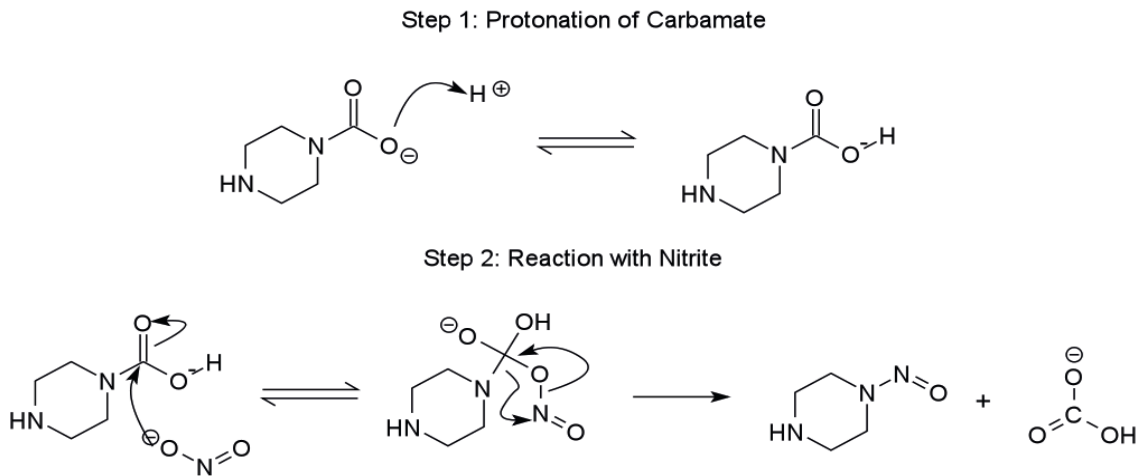


Fig. 3: Mechanism for PZ nitrosation [15, 18]

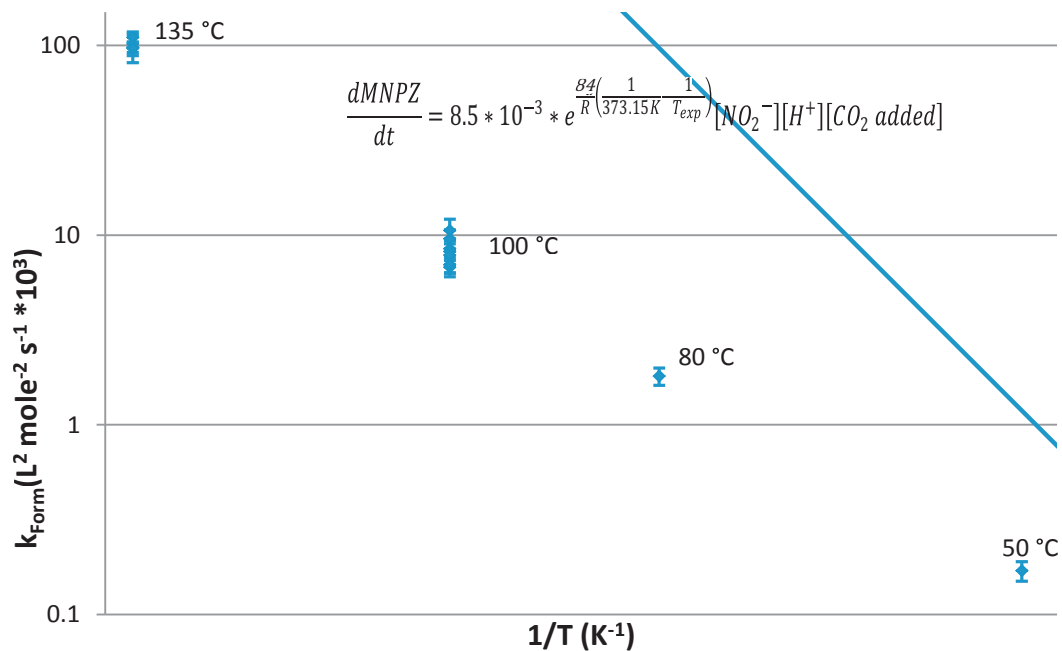


Fig. 4: Temperature dependence of MNPZ nitrosation [18]

Conditions: 0.1–8 m PZ, 0.1–0.4 CO₂ loading, pH controlled with phosphate buffer

4. Thermal Decomposition of MNPZ

MNPZ thermal decomposition was measured using Swagelok thermal cylinders heated to stripper conditions; under these conditions MNPZ decomposition was found to be first order in MNPZ. [19, 20] The pseudo-first order rate constant was analysed with PZ varying from 0.1–8 m and a CO₂ loading of 0.1

and 0.3. The pseudo-first order rate constant can be modelled within 15% of the experimental results for stripper conditions (Equations 5 & 6). Decomposition is not catalyzed by stainless steel ions or stainless steel surface area.

$$k_{Decomp} = 10.2 * 10^{-6} e^{\frac{94 \text{ kJ/mol}}{R} \left(\frac{1}{408} - \frac{1}{T} \right)} * \frac{C_{PZ}^{0.47}}{8m} s^{-1} \quad \text{For } \alpha=0.3 \quad (5)$$

$$k_{Decomp} = 12.2 * 10^{-6} e^{\frac{75 \text{ kJ/mol}}{R} \left(\frac{1}{408} - \frac{1}{T} \right)} s^{-1} \quad \text{For } \alpha=0.1 \quad (6)$$

5. DNPZ Formation and Decomposition

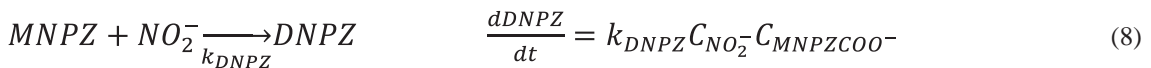
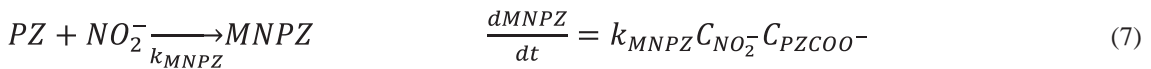
5.1 Experimental Method

A solution of 8 m PZ with 0.3 CO₂ loading was spiked with 50–200 mmol/kg of sodium nitrite (NaNO₂). The solution was loaded into Swagelok thermal cylinders and heated in a vented convection oven for one hour at 150 °C to yield complete conversion of nitrite to nitrosamine. The cylinders were quenched in water and emptied into amber vials to limit further decomposition of the nitrosamine.

The samples were diluted 40x in water and analyzed for MNPZ and DNPZ using HPLC. The calibration curve for DNPZ was created using a 99% pure DNPZ standard purchased from Toronto Research Chemicals. The HPLC method and column was the same used for previous MNPZ experiments. [20] DNPZ elutes between 7.6 and 9 minutes and has a unique bimodal shape (Appendix 1). The calibration curve was linear in the analyzed region with a quantification limit of 0.4 ppm DNPZ and a detection limit of 0.1 ppm DNPZ.

5.2 Kinetics Modeling

DNPZ was hypothesized to form from the nitrosation of the carbamated amine of MNPZ. For a low yield of DNPZ and a reaction time of one hour, the batch rate equations can be modeled as two parallel reactions with no nitrosamine decomposition as shown below. Both k_{MNPZ} and k_{DNPZ} are extremely sensitive to pH.



DNPZ formation is effectively second order in NO₂[−] with the intermediate MNPZ. The solution to Equation 5 is given below along with the final DNPZ yield after complete nitrosation.

$$\frac{C_{DNPZ}}{C_{NO_2^-i}} = \frac{k_{DNPZ}}{2k_{MNPZ}C_{PZCOO^-}} (1 + e^{-2k_{MNPZ}t} - 2e^{-k_{MNPZ}t}) C_{NO_2^-i} \quad (9)$$

$$Yield = \frac{C_{DNPZ}}{C_{NO_2^-i}} = \frac{k_{DNPZ}}{2k_{MNPZ}} * \frac{C_{NO_2^-i}}{C_{PZCOO^-}} \quad (10)$$

5.3 DNPZ Formation Results

The yield was plotted against initial NO_2^- and was linear with a slope of 0.014 kg solution/mol NO_2^- (Figure 5). In a continuous cycle, the concentration of MNPZ will reach a steady state, and the yield to DNPZ will be a constant dependent on the ratio of k_{DNPZ} to k_{MNPZ} . For 8 m PZ with a 0.3 CO_2 loading, the ratio of k_{DNPZ} to k_{MNPZ} is approximately $0.03 \cdot C_{\text{MNPZ}}$.

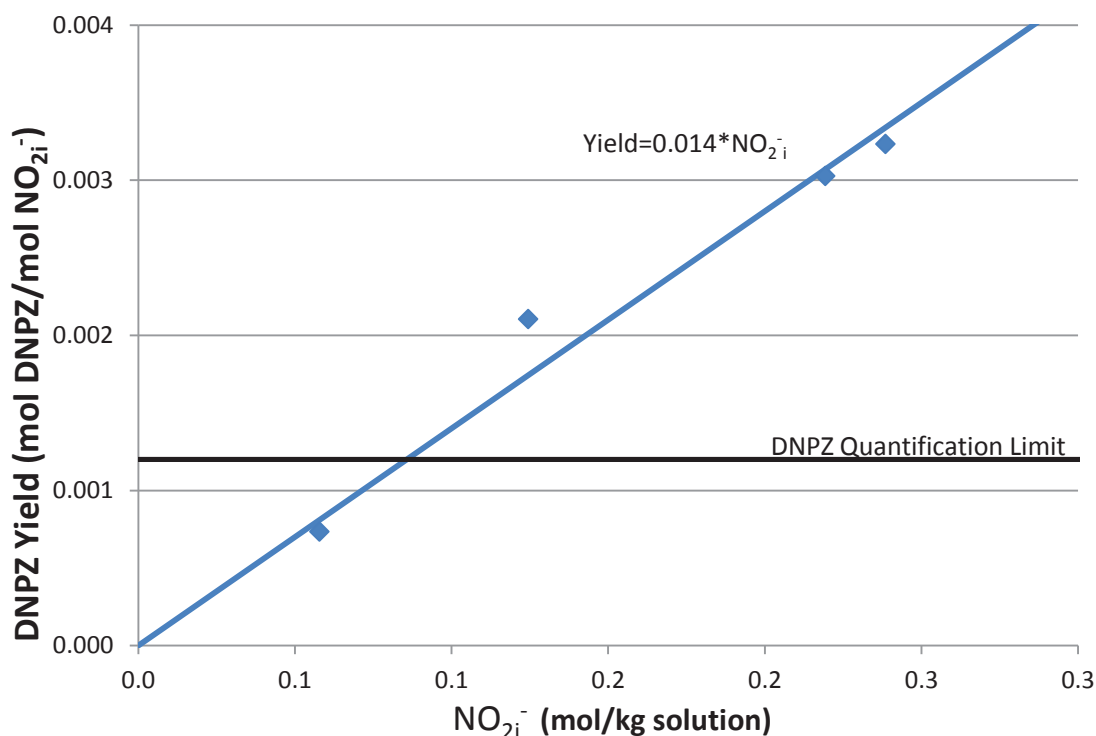


Fig 5: DNPZ yield
Conditions: 8 m PZ, 0.3 CO_2 loading, 150 °C, 1 hour

5.4 DNPZ Decomposition

8 m PZ with 0.3 CO_2 loading was spiked with 5 mmol/kg of DNPZ standard and heated to 150 °C. The DNPZ decomposed below the quantification limit within 16 hours with a pseudo-first order rate constant of $90 \cdot 10^{-6} \text{ s}^{-1}$.

6. Modeling NNO Concentrations in Amine Scrubbing

6.1 Model Development

Modeling MNPZ and DNPZ begins with the NO_2 in the flue gas. A fraction (α) of this NO_2 absorbs into the solvent as NO_2^- while the rest directly reacts to form MNPZ. The NO_2^- then enters the stripper where it nitrosates PZ to form MNPZ and trace amounts of DNPZ with near perfect yield. The non-volatile NNO species and NO_2^- will recycle back to the absorber where they pick up more NO_2^- from the

flue gas (Figure 6). NO_2 in the flue gas is assumed to be the only nitrosating agent for nitrosamine formation, but nitrosating agents from PZ oxidation might become important precursors to nitrosamine formation if the flue gas is scrubbed of NO_2 . [21]

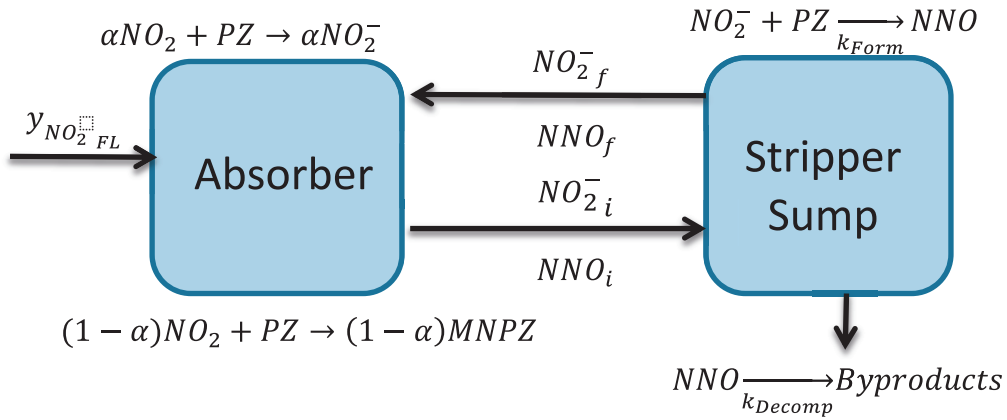


Fig. 6: Nitrite and nitroso-PZ streams in amine scrubbing

Equations 11–14 give overall mole balances across the stripper for NO_2^- and NNO with the stripper sump modeled as an ideal CSTR. NO_2^- approaches steady state in the first hour, so the NO_2^- time derivative is approximated as zero (Equation 8).

$$\dot{n}_{\text{NO}_2^-i} = \dot{n}_{\text{NO}_2^-f} + y_{\text{NO}_2\text{Flue}}G \quad (11)$$

$$\frac{dn_{\text{NO}_2^-}}{dt} = \dot{n}_{\text{NO}_2^-i} - \dot{n}_{\text{NO}_2^-f} - V_{\text{sump}}k_{\text{Form}}C_{\text{NO}_2^-f} \approx 0 \quad (12)$$

$$\dot{n}_{\text{NNO}i} = \dot{n}_{\text{NNO}f} \quad (13)$$

$$\frac{dn_{\text{NNO}}}{dt} = \dot{n}_{\text{NNO}i} - \dot{n}_{\text{NNO}f} + V_{\text{sump}}(k_{\text{Form}}C_{\text{NO}_2^-f} - k_{\text{Decomp}}C_{\text{NNO}f}) \quad (14)$$

Dividing by the total volume of the amine scrubber and simplifying yields Equation 15.

$$\frac{dC_{\text{NNO}}}{dt} = \frac{y_{\text{NO}_2\text{Flue}}G}{V_{\text{tot}}} - \frac{V_{\text{sump}}}{V_{\text{tot}}}k_{\text{Decomp}}C_{\text{NNO}f} \quad (15)$$

Solving gives the time-dependent and steady state NNO concentration, which is almost entirely MNPZ (Equations 16 & 17).

$$\text{MNPZ}(t) = \text{MNPZ}_i + (\text{MNPZ}_{\text{SS}} - \text{MNPZ}_i)[1 - e^{-k_{\text{Decomp}}\frac{V_{\text{sump}}}{V_{\text{tot}}}t}] \quad (16)$$

$$\text{MNPZ}_{\text{SS}} = \frac{y_{\text{NO}_2\text{Flue}}G}{k_{\text{Decomp}}V_{\text{sump}}} = \frac{y_{\text{NO}_2\text{Flue}}}{k_{\text{Decomp}}\tau_{\text{sump}}} * \frac{G}{L} \quad (17)$$

Formation of the NNO can be modelled as two parallel reactions to give the yield of DNPZ for a steady-state MNPZ concentration (Equation 18).

Since the ratio of MNPZ to PZ is so low, the yield of DNPZ is expected to be very small.

$$\frac{DNPZ_{ss}}{MNPZ_{ss}} = \frac{C_{MNPZ} k_{Form DNPZ}}{C_{PZ} k_{Form MNPZ}} * \frac{k_{Decomp MNPZ}}{k_{Decomp DNPZ}} \quad (18)$$

6.2 Pilot Plant comparison

A concentrated PZ solvent from a pilot plant running a real flue gas was sampled over an extended period of time and analyzed for MNPZ and DNPZ. Figure 5 shows MNPZ concentration from the pilot plant along with the modeled MNPZ at conditions similar to the pilot plant conditions. MNPZ reached a steady state concentration between 1 mM and 2 mM. It takes on the order of 10 days for MNPZ to reach a new steady state concentration after a step change to the parameters. The steady state DNPZ will be on the order of 10^{-8} M, which is undetectable using current methods.

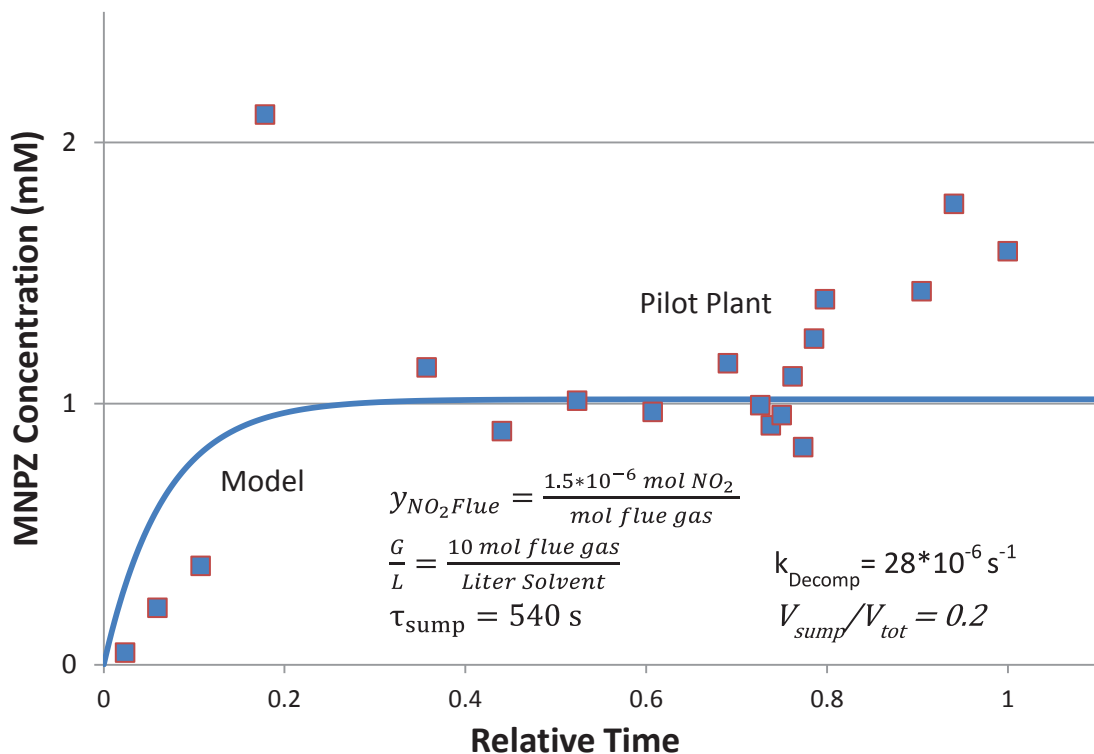


Fig. 7: Comparison of Pilot Plant MNPZ and Model

7. Conclusions

- The k_g is approximately 10^{-6} mol/Pa·m²·s for NO₂ absorption in 8 m PZ at 40 °C.
- Over 90% of the NO₂ will absorb as NO₂⁻ or MNPZ.

- MNPZ formation from NO_2^- is first order in NO_2^- , PZCOO^- , and H^+ .

$$\frac{d\text{MNPZ}}{dt} = 8.9 * 10^{-3} * e^{\frac{84}{R} * (\frac{1}{373} - \frac{1}{T})} [\text{NO}_2^-] [\text{H}^+] [\text{R}_2\text{NCOO}^-]$$

- MNPZ decomposition is first order in MNPZ and dependent on PZ and CO_2 loading.

$$k_{\text{Decomp}} = 10.2 * 10^{-6} e^{\frac{94 \text{ kJ/mol}}{R} (\frac{1}{408} - \frac{1}{T})} * \frac{C_{\text{PZ}}^{0.47}}{8m} \text{ s}^{-1} \quad \text{For } \alpha=0.3$$

$$k_{\text{Decomp}} = 12.2 * 10^{-6} e^{\frac{75 \text{ kJ/mol}}{R} (\frac{1}{408} - \frac{1}{T})} \text{ s}^{-1} \quad \text{For } \alpha=0.1$$

- DNPZ formation is first order in NO_2^- and MNPZ.
- MNPZ formation will balance out with MNPZ thermal decomposition to yield a steady state MNPZ concentration that is on the order of 1 mM.

$$\text{MNPZ}_{ss} = \frac{y_{\text{NO}_2\text{Flue}} G}{k_{\text{Decomp}} V_{\text{sump}}} = \frac{y_{\text{NO}_2\text{Flue}}}{k_{\text{Decomp}} \tau_{\text{sump}}} * \frac{G}{L}$$

- Reaching the steady state concentration takes on the order of 10 days.

$$\text{MNPZ}(t) = \text{MNPZ}_i + (\text{MNPZ}_{ss} - \text{MNPZ}_i) [1 - e^{-k_{\text{Decomp}} \frac{V_{\text{sump}}}{V_{\text{tot}}} * t}]$$

- The concentration of DNPZ is on the order of 10^{-5} mM, which is undetectable using current methods.

$$\frac{\text{DNPZ}_{ss}}{\text{MNPZ}_{ss}} = \frac{C_{\text{MNPZ}} k_{\text{Form DNPZ}}}{C_{\text{PZ}} k_{\text{Form MNPZ}}} * \frac{k_{\text{Decomp MNPZ}}}{k_{\text{Decomp DNPZ}}}$$

Acknowledgements

This work was supported by the Luminant Carbon Management Program at the University of Texas at Austin.

References

- [1] Freeman, S. A.; Dugas, R. E.; Van Wagener, D. H.; Nguyen, T.; Rochelle, G. T. Carbon dioxide capture with concentrated, aqueous piperazine. *Int. J. Greenh. Gas Con.* 2010, 4, 119–24; DOI: 10.1016/j.ijggc.2009.10.008.
- [2] Douglass, M. L. The chemistry of nitrosamine formation, inhibition and destruction. *J. Soc. Cosmet. Chem.* 1978, 29, (9), 581–606.
- [3] Lijinsky, W.; Conrad, E.; Van De Bogart, R. Carcinogenic Nitrosamines formed by Drug/Nitrite Interactions. *Nature.* 1972, 239, 165–7.
- [4] Mitch, William. Gassnova Website; http://www.gassnova.no/frontend/files/CONTENT/Rapporter/NitrosamineandNitramineformationchemistry_YALE.pdf.
- [5] Garcia, H.; Keefer, L.; Lijinsky, W.; Wenyon C. E. M. Carcinogenicity of nitrosothiomorpholine and 1-nitrosopiperazine in rats. *Cancer Res. Clin. Oncol.* 1970, 74, (2), 179–184; DOI: 10.1007/BF00525883.
- [6] Pai, S. R.; Shirke, A. J.; Gothoskar, S. V. Long-term feeding study in C17 mice administered saccharin coated betel nut and 1,4-dinitrosopiperazine in combination. *Carcinogenesis.* 1981, 2 (3), 175–7.
- [7] Norwegian Climate and Pollution Agency. Permit for activities pursuant to the Pollution Control Act. CO_2 Technology Centre Mongstad DA. 2011.
- [8] Chen, S. Nitrogen Dioxide Absorption in Aqueous Sodium Sulfite. Ph.D. Dissertation, The University of Texas Austin, Austin, TX, 1997.
- [9] Mimura, T.; Shimojo, S.; Iijima, M.; Mitsuoka, S. Process for Removing Carbon Dioxide and Nitrogen Oxides from Combustion Gases. U.S. Patent 5,648,053, July 15, 1997.
- [10] Dai, N., Shah, A. D., Hu, L., Plewa, M. J., Mckague, B., & Mitch, W. A. (2012). Measurement of Nitrosamine and Nitramine Formation from NO_x Reactions with Amines during Amine-Based Carbon Dioxide Capture for Postcombustion Carbon Sequestration. *Environmental Science and Technology*, 46, 9793–9801.

- [11] Challis, B. C.; Kyrtopoulos, S. A. Chemistry of Nitroso- Compounds. 11. Nitrosation of amines by the 2-phase interaction of amines in solution with gaseous oxides of nitrogen. *J. Chem. Soc., Perkin Trans. 1* 1979, 2, 299–304.
- [12] Mirvish, S. S. N - nitroso compounds: Their chemical and in vivo formation and possible importance as environmental carcinogens. *J. Toxicol. Environ. Health*. 1977, 2, 1267 – 77.
- [13] Zhao, Y-L.; Garrison, S. L.; Marquez, M. N-Nitrosation of Amines by NO₂ and NO: A Theoretical Study. *J. Phys. Chem. A*. 2007, 111 (11), 2200–2205; DOI: 10.1021/jp0677703.
- [14] Casado, J.; Mosquera, M.; Paz, L. C.; Prieto, M. F. R.; Tato, J. V. Nitrite Ion as a Nitrosating Reagent. Nitrosation of Morpholine and Diethylamine in the Presence of Formaldehyde. *J. Chem. Soc., Perkin Trans. 2*. 1984, 12, 1963–66; DOI: 10.1039/P29840001963.
- [15] Sun, Z.; Liu, Y. D.; Zhong, R. G. Carbon Dioxide in the Nitrosation of Amine: Catalyst or Inhibitor? *J. Phys. Chem. A*. 2011, 115 (26), 7753–64; DOI: 10.1021/jp202002m.
- [16] Sexton, A. J.; Rochelle, G.T. Oxidation products of amines in CO₂ capture. *Proceedings of Greenhouse Gas Technologies* 8, Trondheim, Norway, 2006. pp 1–6.
- [17] Dugas, R.E. "Carbon Dioxide Absorption, Desorption, and Diffusion in Aqueous Piperazine and Monoethanolamine." Ph.D. Dissertation, The University of Texas Austin, Austin, TX, 2009.
- [18] Goldman, M.; Fine, N.A.; Rochelle, G.T. Formation of N-Nitrosopiperazine in the CO₂ capture process. Manuscript in preparation for submission to *Env. Sci. & Tech.*, 2012.
- [19] Ashouripashaki, M. Formation and Decomposition of 1-Nitrosopiperazine in the CO₂ Capture Process. M.S. Thesis, The University of Texas Austin, Austin, TX, 2012.
- [20] Fine, N.A.; Rochelle, G.T. Thermal Decomposition of N-nitrosopiperazine. Presented at GHGT-11, Kyoto, Japan, November 18–22, 2012. *Energy Procedia*, 2013.
- [21] Nielsen, P. T.; Li L.; Rochelle G.T. Piperazine degradation in pilot plants. Presented at GHGT-11, Kyoto, Japan, November 18–22, 2012. *Energy Procedia*, 2013.

Appendix 1. DNPZ elution on HPLC

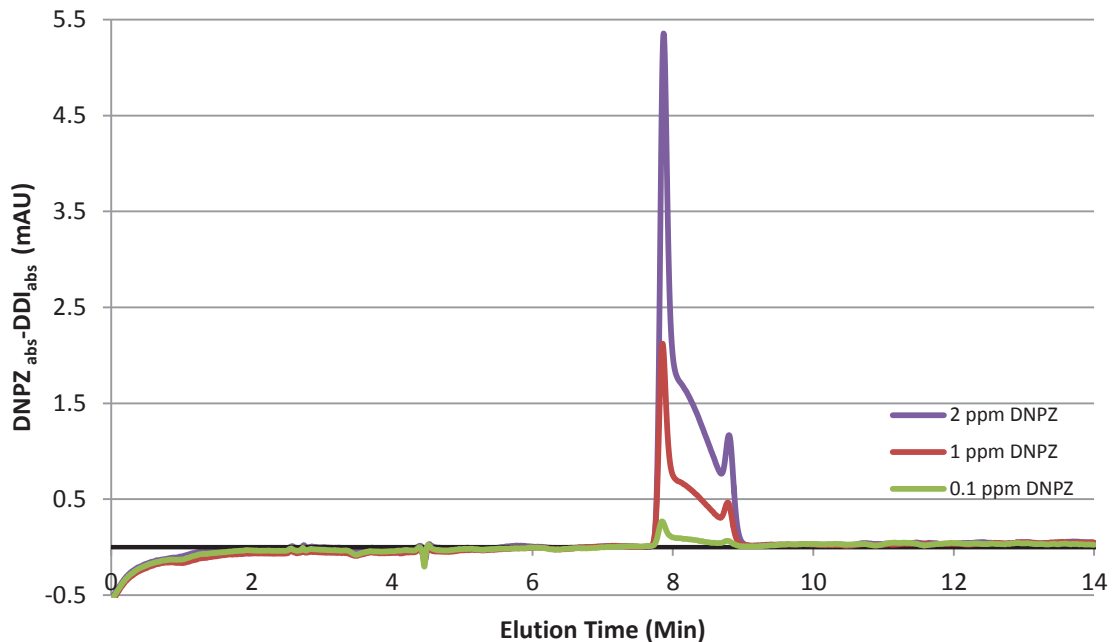


Fig. 8: DNPZ elution time and peak shape using HPLC

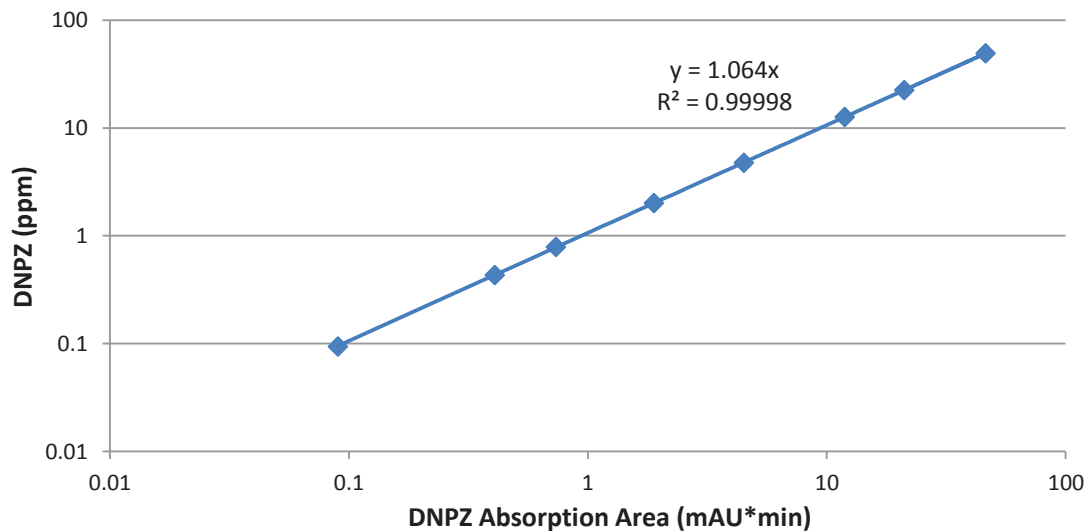


Fig. 9: DNPZ Quantification using HPLC

Column: AcclaimTM PolarAdvantage II column, 4.6mm x 500mm

Eluents: 10 mM ammonium carbonate (pH=9.1) polar phase, Acetonitrile non-polar phase

Eluent Composition: 95% (NH₄)₂CO₃ and 5% ACN from 0-10 min.; 50% (NH₄)₂CO₃ and 50% ACN from 10-14 min.

Eluent Flow: 1 mL/min

UV wavelength: 240 nm